NASA TECHNICAL NOTE

NASA TN D-1587

c. 1

NASA TN D-1587

NEUTRON SELF-SHIELDING FACTORS FOR MULTIPLE-BODY CONCENTRIC CYLINDRICAL CONFIGURATIONS

by Thor T. Semler

Lewis Research Center
Cleveland, Ohio

NATIONAL AERONAUTICS AND SPACE ADMINISTRATION • WASHINGTON, D. C. • SEPTEMBER 1964

NEUTRON SELF-SHIELDING FACTORS FOR MULTIPLE-BODY CONCENTRIC CYLINDRICAL CONFIGURATIONS

By Thor T. Semler

Lewis Research Center
Cleveland, Ohio

NATIONAL AERONAUTICS AND SPACE ADMINISTRATION

For sale by the Office of Technical Services, Department of Commerce,
Washington, D.C. 20230 -- Price $0.50

NEUTRON SELF-SHIELDING FACTORS FOR MULTIPLE-BODY CONCENTRIC CYLINDRICAL CONFIGURATIONS

by Thor T. Semler

Lewis Research Center

SUMMARY

Monte Carlo calculations of the self-shielding factors for multiple-body concentric cylindrical geometries are made and the results are compared with the rational approximation and other analytic results. The blackness for a monoenergetic neutron flux incident upon an infinite length cylindrical shell of absorber with central internal rods of absorber and multiple concentric ring configurations are calculated by means of the Monte Carlo method. A cosine incident-angular-neutron distribution and one collision model are chosen. The probability of absorption is calculated for thin shell and central rod combinations and for multiple concentric cylinders for a range of macroscopic absorption cross sections.

The self-shielding factors computed for these configurations are compared with the results of the rational approximation as well as other analytic results. For large variations in internal structure the self-shielding factors show large deviations from the rational approximation and from exact calculations for equivalent solid rods. For multiple concentric annuli, however, the correlation of self-shielding factor with volume-to-surface ratio is quite precise and agrees with the corresponding equivalent solid rod.

To further illustrate the technique, a Monte Carlo calculation is made for the blackness of arrays of concentric cylinders for a single Breit Wigner resonance absorber exposed to a neutron slowing-down distribution.

INTRODUCTION

In the design of heterogeneous nuclear reactors it is essential to have convenient and accurate means for estimating self-shielding effects. If the geometry of the region for which the self-shielding factor is sought is moderately complex, the calculation of this parameter becomes difficult if not impossible to compute by analytic means. For lumped absorbers of arbitrary shape and mass distribution, various approximations (refs. 1 and 2) have been used with varying degrees of success. Perhaps the most widely used approximation has been the rational approximation of Wigner, et al. (ref. 2). The rational approximation asserts that, for a spatially uniform isotropic source of neutrons in a volume V, the escape probability P_o may be estimated by the formula

$$P_o = \frac{1}{1 + \Sigma_t \frac{4V}{S}}$$

where Σ_t is the total macroscopic cross section and V/S is the volume-to-surface ratio of the lump with 4V/S corresponding to the average chord length. The rational approximation, however, is subject to as much as 18 percent error (ref. 1) for cylindrical rods. The error associated with the use of the rational approximation to determine the self-shielding of cylindrical shells is likewise rather large. The precision of available methods for the calculation of self-shielding factors for a configuration of concentric cylindrical shells is unknown. The present calculations have been made by Monte Carlo methods to ascertain the validity of the correlation of the V/S ratio to the self-shielding factor for large variations in the internal structure of infinitely long multiple-body concentric cylindrical configurations. To further illustrate the utility of the Monte Carlo technique, a blackness factor averaged over a single-level Breit-Wigner resonance is computed for an array of concentric hollow cylinders.

A Monte Carlo Fortran IV code that conveniently handles complex cylindrical geometries has been written and used in the present analysis. A nonscattering model has been used with a cosine angular-neutron-flux distribution incident upon the cylindrical arrays.

SYMBOLS

E	energy, ev
E_{min}, E_{max}	minimum and maximum energy considered
E_{neu}	energy of neutron
F_s	self-shielding factor
f	optical length through cylinder
m	number of annuli
N_r	r^{th} random number whose range is 0.0 to 1.0
n	number of neutron histories
P	probability of nontransmission
P_o	escape probability
R	distance from point to center of cylindrical assembly

R_1 outside radius of shell

R_2 inside radius of shell

R_3 radius of internal rod

R_4 outside radius of single annulus (fig. 11)

R_5 inside radius of single annulus (fig. 11)

r_{2i} outside radius of i^{th} annulus

r_{2i-1} inside radius of i^{th} annulus

r_{2m} outside radius of annular configuration of m annuli

S outside surface area exposed per unit length

S_a outside surface area exposed per unit length for annular configuration

T probability of transmission

t thickness of thin shell in thin shell and internal rod configuration

V volume of absorbing material per unit length

V_A volume of absorbing material per unit length in multiple annuli configuration

δ error

θ angle between diameter through source and projection of neutron trajectory on plane orthogonal to axis of symmetry through source

θ_1 angle between diameter and tangent to inside of hollow shell (see fig. 2)

$\vec{\theta}_u$ unit vector in θ direction

λ total path length to collision

λ_p projection of path length to collision on cutting plane

μ mean

ξ $\left(\frac{2V}{S}\right)\Sigma_a$

Σ_a macroscopic absorption cross section

Σ_t total macroscopic cross section

σ_s standard deviation

Φ angle between neutron trajectory and projection of neutron trajectory on plane orthogonal to axis of symmetry through source

$\vec{\Phi}_u$ unit vector in Φ direction

φ_s neutron flux at surface of cylinder

$\bar{\varphi}$ average flux within body

ANALYSIS

The Monte Carlo program assumes a nonscattering model, that is, each collision constitutes an absorption. The cross sections used are either monoenergetic or correspond to single-level resonances. The ratio of the number of absorbed neutrons to the total number of neutrons incident, which is the blackness of the configuration, is calculated and appears as output from the Monte Carlo program; from the calculated blackness of a configuration one may calculate the self-shielding factor.

An outline (fig. 1) chronologically associated with the flow diagram of the Monte Carlo techniques used in this program will be followed in the analysis. A neutron is generated with energy taken randomly from the neutron energy distribution $1/E$ in the interval from the minimum energy to the maximum energy considered. The following rejection technique is used to produce this distribution. First a neutron energy is chosen in the energy interval from E_{min} to E_{max} by the following formula:

$$E_{neu} = E_{min} + N_r(E_{max} - E_{min})$$

Next the value of N_{r+1} is compared to the value of the following expression:

$$\frac{E_{min}}{E_{neu}} = \frac{\frac{1}{E_{neu}}}{\frac{1}{E_{min}}}$$

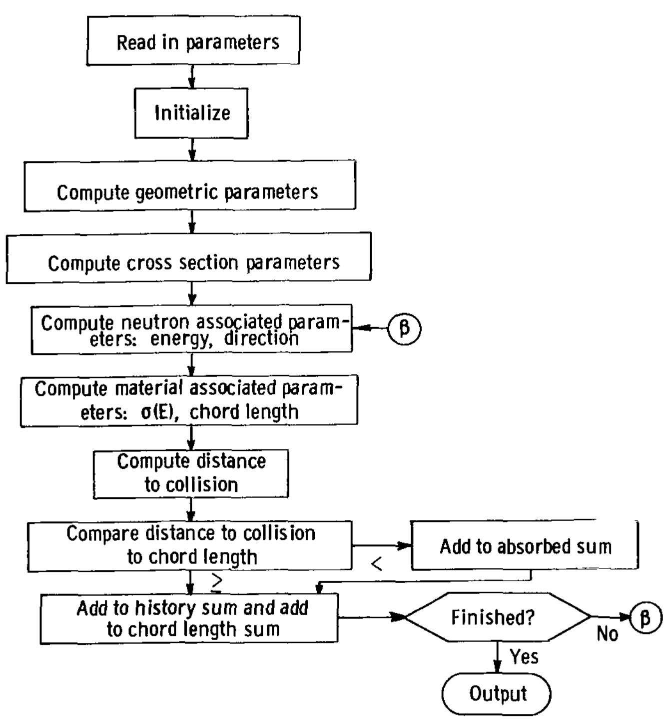

Figure 1. - Generalized flow chart.

If the value of N_{r+1} is less than or equal to the value of the expression, the value is accepted; otherwise the value E_{neu} is rejected and the entire process is repeated. The average of the process checked against the expectation value is found to give excellent agreement, better than 0.1 percent for ten thousand histories.

A cosine angular distribution of the incident-neutron number flux is used as well as an isotropic incident-neutron distribution. The method used to generate these distributions is similar to that of Cashwell (ref. 3). The expressions used are derived in appendix A.

An option of the program allows a constant cross section or resonance parameter to be read in. When the single-level resonance absorption cross sections are used, Doppler broadening is neglected, and the cross sections are computed from the standard Breit-Wigner formula (refs. 4 and 5). In computing the blackness over a representative Breit-Wigner resonance, a maximum energy and a minimum energy are chosen. The program computes a blackness averaged over a $1/E$ neutron energy spectrum. The path length to collision is calculated in the usual manner

$$\lambda = -\frac{\ln N_r}{\Sigma_t}$$

The thickness of material seen by the neutron (the optical thickness) f is then calculated. This thickness of material is compared with the length λ. If λ is longer than f, the neutron is not absorbed. If λ is less than or equal to f, the neutron is absorbed. The value of f for the hollow cylinder is computed from

$$f = \frac{2\left[R_1 \cos \theta - (R_2^2 - R_1^2 \sin \theta)^{1/2}\right]}{\cos \Phi}$$

and for the thin shell and rod (fig. 2) from

$$f = \frac{2\left[R_1 \cos \theta - (R_2^2 - R_1^2 \sin^2\theta)^{1/2} + (R_3^2 - R_1^2 \sin^2\theta)^{1/2}\right]}{\cos \Phi}$$

The derivation of these expressions is shown in appendix B.

A self-shielding factor F_s is defined to be the ratio of the average flux inside a body to the surface flux (ref. 6)

$$F_s = \frac{\bar{\varphi}}{\varphi_s}$$

The inwardly directed current or number of neutrons per second striking a body immersed in an isotropic scattering medium is $\varphi_s S/4$, where S is the outside surface area of the body containing material of volume V and of macroscopic absorption cross section Σ_a. If T is the fraction of the incident neutrons leaving the assembly, the blackness $1 - T$ is given by

$$1 - T = \frac{\Sigma_a \bar{\varphi} V}{\frac{\varphi_s S}{4}} = \frac{\Sigma_a V}{\frac{S}{4}} F_s$$

or

$$F_s = \frac{1 - T}{\Sigma_a \frac{4V}{S}} = \frac{1 - T}{2\xi}$$

where

$$\xi = \frac{2\Sigma_a V}{S}$$

Configurations

Hollow cylinder and shell and rod configuration. - Self-shielding calculations are made for two geometric configurations. The thin cylinder with an internal rod shown in figure 2 and the hollow cylinder are chosen because they represent two extremes of internal structure. Since these configurations are not completely specified by the parameter ξ, a particular family is chosen to illustrate the differences in self-shielding factors. The surface area exposed per unit length is the same for both configurations. The internal volume and density of absorber per unit length of both assemblies is held constant for each value of ξ.

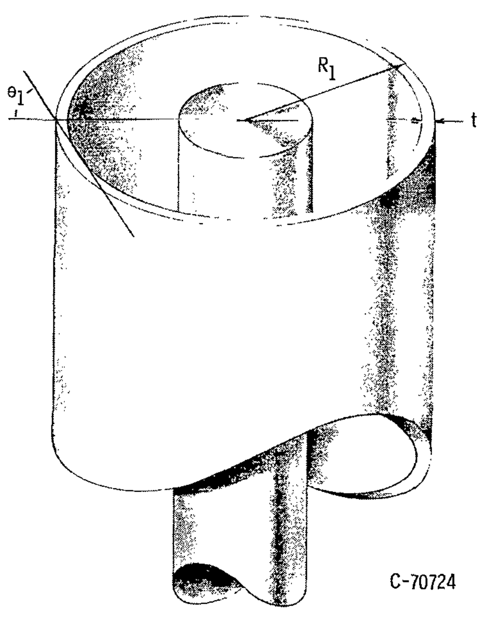

Figure 2. - Thin cylinder with internal rod configuration.

For a hollow cylinder of outside radius R_1, it is shown in reference 7 that

$$\xi = R_1 \Sigma_a \cos^2\theta_1$$

where θ_1 is the angle between a diameter and a line tangent to the inside wall of the hollow cylinder (see fig. 2). Thus, to vary ξ, one can vary either the outside radius, the macroscopic absorption cross section, or the amount of material inside the shell. The hollow cylinders calculated used the product $R_1\Sigma_a = 1.0$, a constant; thus, to vary ξ, the amount of material inside the hollow shell is changed, that is, the central hollow gradually is filled with material. As $\theta_1 \rightarrow 0$, $\xi \rightarrow 1.0$; for $\xi = 1.0$, under the foregoing conditions, a solid rod is obtained.

The thin shell and rod cases shown in figure 2 used constant values of the ratio of shell thickness to outside radius t/R_1 of 0.0005 and 0.05. The difference in mass between the thin shell and the hollow cylinder configuration appeared as the central rod of the thin shell and the central rod configuration. Representative values of dimensions are shown in table I.

Multiple-body concentric cylindrical configurations. - Self-shielding calculations are made for a series of concentric shells illustrated in figure 3. The number of shells making up the assembly is a parameter varied from 1 to 20; the ratio of shell material volume to outside surface V/S is held constant. The volume per unit length of the annuli is given by

$$V_A = \pi \sum_{i=1}^{m} (r_{2i} + r_{2i-1}) \times (r_{2i} - r_{2i-1})$$

where m is the number of annuli, r_{2i} is the outside radius of the i^{th} shell, and r_{2i-1} is the inside radius of the i^{th} shell.

TABLE I. - REPRESENTATIVE DIMENSIONS FOR HOLLOW CYLINDERS AND THIN SHELLS WITH INTERNAL RODS

Hollow cylinder			Thin shell and internal rod	
Surface-to-volume ratio of lump, S/V, cm^{-1}	Outside radius of hollow cylinder, R_1, cm	Radius of inner hollow shell, R_2, cm	Ratio of shell thickness to outside radius, t/R_1	Radius of internal rod, R_3, cm
2000	1.000	0.9995	0.0005	-------
1667	↓	.9994	↓	0.01414
1000		.9990		.03161
500		.9980		.05474
250		.9960		.08357
100		.9900		.13748
50		.9800		.19647
25		.9600		.27821

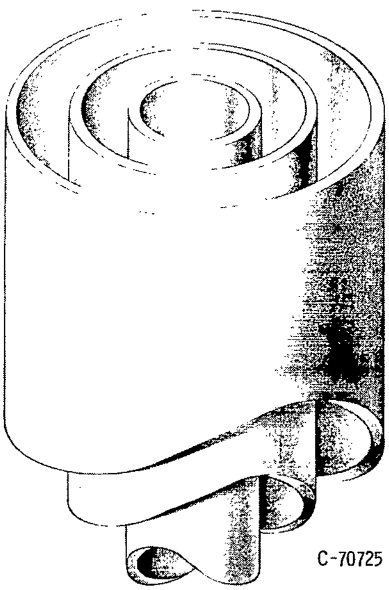

Figure 3. - Concentric cylindrical annuli configuration.

The outside surface area per unit length is

$$S_a = 2\pi r_{2m}$$

The volume-to-surface ratio is

$$\frac{V}{S} = \frac{V_A}{S_a} = \frac{\sum_{i=1}^{m} (r_{2i} + r_{2i-1})(r_{2i} - r_{2i-1})}{2r_{2m}}$$

and

$$\xi = \left(\frac{2V}{S}\right)\Sigma_a = \left[\frac{\sum_{i=1}^{m} (r_{2i} + r_{2i-1})(r_{2i} - r_{2i-1})}{r_{2m}}\right]\Sigma_a$$

For a given ξ there is a rather varied choice of geometries; that is, ξ does not completely specify an annular cylindrical geometry. The following ancillary conditions were added to specify the geometry of the annuli.

(1) The cylindrical thickness for a given configuration containing m cylinders shall be equal; that is,

$$r_{2i} - r_{2i-1} = t \qquad (i = 1,2,3,\ldots,m)$$

(2) The spacing between cylinders for a given m shall be equal. For example, the distance from the z-axis of symmetry to the outside of ring 1 is just one-half that to the outside of ring 2.

(3) The ratio V/S is held constant, while the number of rings is allowed to vary.

(4) For a given m and V/S, Σ_a is varied to change the value of ξ.

(5) The outside radius of all concentric cylindrical configurations considered herein is chosen at 1.5 inches.

TABLE II. - DIMENSIONS OF MULTIPLE CONCENTRIC CYLINDERS

Number of rings	Outside radius of configuration, cm	Thickness of annuli, cm	Spacing of annuli (outside radius to outside radius), cm
20	3.81	0.0240	0.1905
10	↓	.0461	.3810
6	↓	.0728	.6350
4	↓	.1024	.9525
3	↓	.1280	1.2700
2	↓	.1720	1.9050
1	↓	.2590	------

The foregoing conditions specify the concentric ring geometries. The values of the radii chosen are shown in table II. The values of m, ξ, and F_s are shown in table III. A cosine incident angular neutron number flux is used.

Concentric Cylinders of Resonance Absorbers

The Monte Carlo program is also executed for a representative resonance (Ag^{109} at 5.20 ev) (see ref. 4). Values of the radii chosen are shown in table IV. To illustrate the sensitivity of the results to incident-angular-flux distributions, an isotropic incident-neutron case was also calculated.

TABLE III. - SELF-SHIELDING FACTORS FOR CYLINDRICAL CONFIGURATIONS

Number of rings	Values of ξ^a				
	0.10	0.20	0.30	0.40	0.50
1	0.875(0)	0.775(2)	0.696(3)	0.631(6)	0.574(0)
2	.885(5)	.789(2)	.708(6)	.642(0)	.584(9)
3	.900(7)	.796(9)	.713(3)	.645(7)	.587(4)
4	.891(5)	.796(1)	.720(4)	.652(1)	.589(8)
6	.891(4)	.797(2)	.719(1)	.651(1)	.594(5)
10	.894(5)	.804(2)	.721(8)	.652(0)	.593(9)
20	.902(5)	.802(9)	.720(3)	.650(0)	.594(2)
∞	.88502	.79303	.71649	.65162	.59595

[a]Cosine incident.

Statistical Analysis

Given a neutron, there is a probability T that it shall be transmitted through the assembly and a probability P = 1 - T that it will not be transmitted. Let n stochastically independent neutrons be injected into the system; then, x neutrons will be transmitted. These are precisely the postulates necessary for the generation of a binomial distribution (ref. 8).

TABLE IV. - DIMENSIONS OF RESONANCE CONFIGURATION

Number of rings	Outside radius of configuration, cm	Thickness of annuli, cm	Spacing of annuli (outside radius to outside radius), cm
20	1.000	0.0005236	0.0500000
18	↓	.0005787	.0555556
16		.0006469	.0625000
14		.0007332	.0714286
12		.0008461	.0833333
10		.0010000	.1000000
8		.0012224	.1250000
6		.0015721	.1666667
5		.0018345	.2000000
4		.0022019	.2500000
3		.0027532	.3333333
2		.0036723	.5000000
1		.0055102	--------

In order to calculate the first two moments of the binomial distribution, the following formulas are used:

$$\mu = nT$$

where μ is the mean and

$$\sigma_s = \sqrt{nTP}$$

where σ_s is the standard deviation. Thus, the best estimate of T is

$$T = \frac{\mu}{n}$$

and the best estimate of σ_s is

$$\sigma_s = \sqrt{\mu P}$$

Hence, the fractional error associated with one standard deviation is

$$\frac{\sigma_s}{\mu} = \frac{\sqrt{nTP}}{nT} = \sqrt{\frac{P}{nT}}$$

Since

$$F_s = \frac{1 - T}{\Sigma_a \frac{4V}{S}}$$

The fractional error of F_s is

$$\frac{\delta F_s}{F_s} = \frac{1}{\Sigma_a \frac{4V}{S}} \frac{\delta T}{T}$$

For example, if $n = 10{,}000$, $T = 0.75$, and $\left[\Sigma_a(4V/S)\right]^{-1} = 3.33$,

$$\frac{\delta F_s}{F_s} = \left(\Sigma_a \frac{4V}{S}\right)^{-1} \sqrt{\frac{P}{nT}}$$

$$= 3.33 \times 0.57 \text{ percent}$$

$$= 1.90 \text{ percent}$$

Hence 1.90 percent is the percentage error associated with one standard deviation. The errors given to the Monte Carlo results have been calculated in this manner and are standard deviations. These standard deviations are somewhat smaller than the symbols marking the data unless otherwise shown.

RESULTS AND DISCUSSION

Self-shielding factors calculated for two extreme geometric configurations, the thin cylinder with an internal rod and the hollow cylinder (see fig. 2, p. 6) are presented in figure 4 as a function of ξ. A large difference in F_s for these cases is obtained at the smaller values of ξ. These

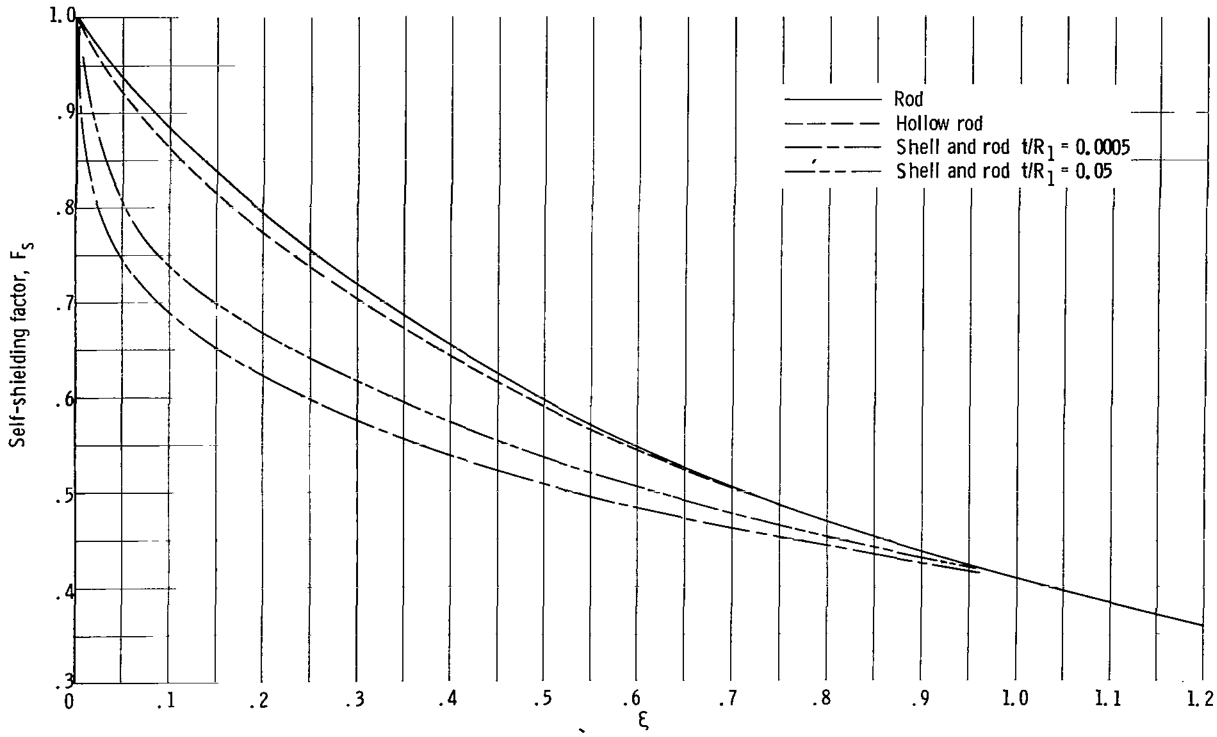

Figure 4. - Self-shielding factors for cylindrical configurations with cosine incident angular flux.

calculated values are compared with exact results for rods (refs. 7 and 9). For the chosen geometries, the configurations correspond to rods at $\xi = 1$ and cross the exact solution here.

The hollow cylinder has its mass concentrated toward its periphery, while the thin cylinder and internal rod has its mass concentrated near the center of the structure; for a cosine incident-angular-flux distribution, therefore, the average chord length is longer for the latter case, and thus the self-shielding effect is greater. (As can be seen from figure 4, the largest discrepancy in the correlation lies in the range $0.00 < \xi \leq 0.50$.) It is evident that the parameter $\xi = (2V/S)\Sigma_a$ does not correlate the self-shielding factors in cylindrical configurations with large variations of internal structure.

For multiple body concentric cylinders, results are shown in figures 5 and 6 for the range $\xi = 0.00$ to $\xi = 0.50$. As noted before, the annuli are chosen all of the same thickness and equally spaced. The outside diameter, a constant, chosen for the outermost annulus was 3.0 inches. The annular dimension remained a constant (see table II, p. 8), and the cross section Σ_a was

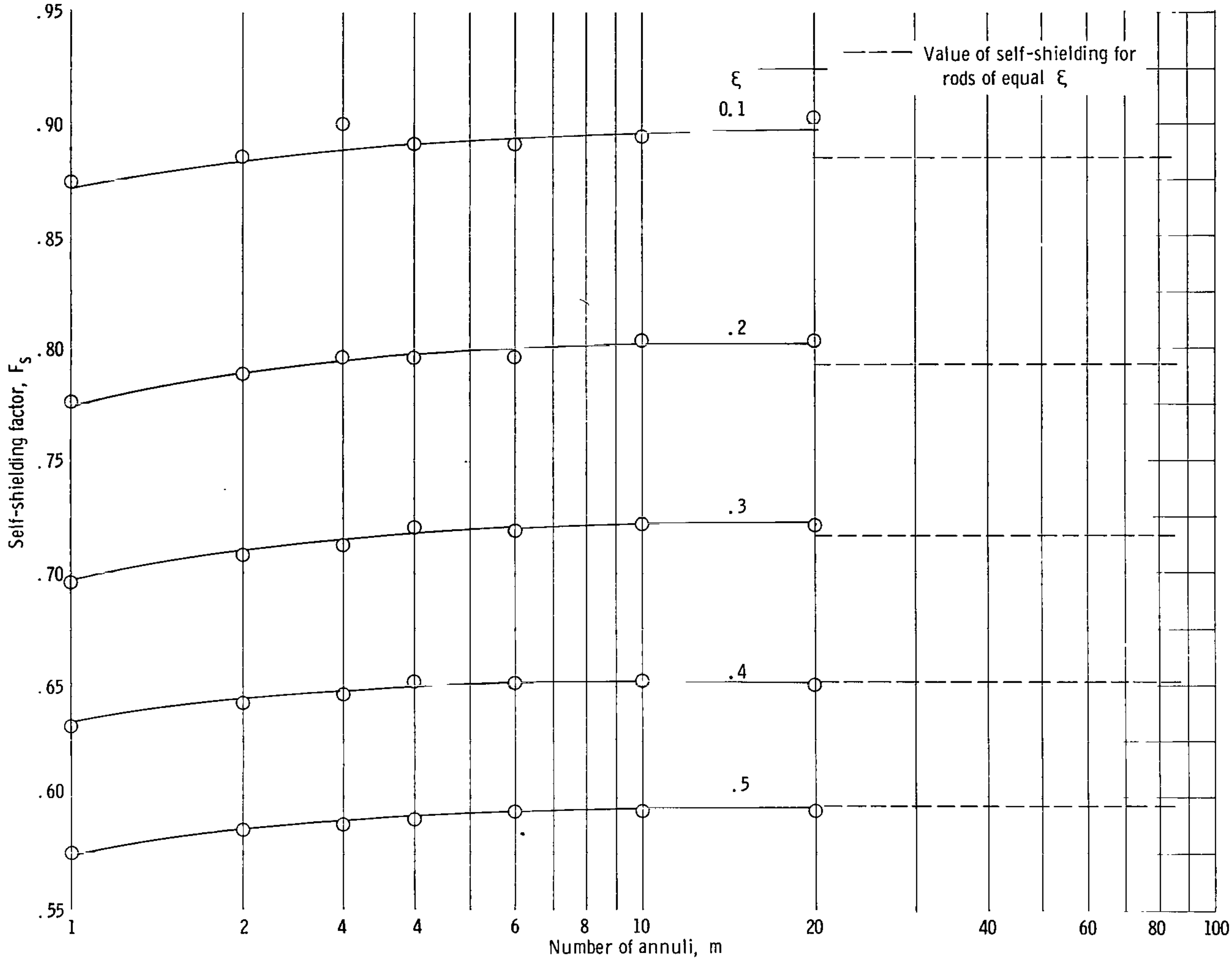

Figure 5. - Self-shielding factors plotted against number of annuli.

varied to change ξ. Results for F_S are shown in table III. As can be seen in figure 5, the self-shielding factors tend to approach the solid rod asymptote for large values of ξ. For low values of ξ, the self-shielding curves for multiple annuli exceed the solid rod asymptote. This effect may well be due to streaming across the internal voids. As the blackness of the array is increased, this effect ceases to be important. For large numbers of rings, the curves approach the self-shielding factors for rods. It appears that, for the range of variables studied, the self-shielding factors for the multiple concentric cylinders is reasonably well approximated by the equivalent solid rod self-shielding factors as prescribed by the ξ correlation.

The results shown in figure 7 present the blackness factors averaged over a Breit-Wigner resonance and a $1/E$ neutron energy distribution. The value of V/S is kept constant at 0.0055 centimeter and the number of cylinders is varied from 1 to 20.

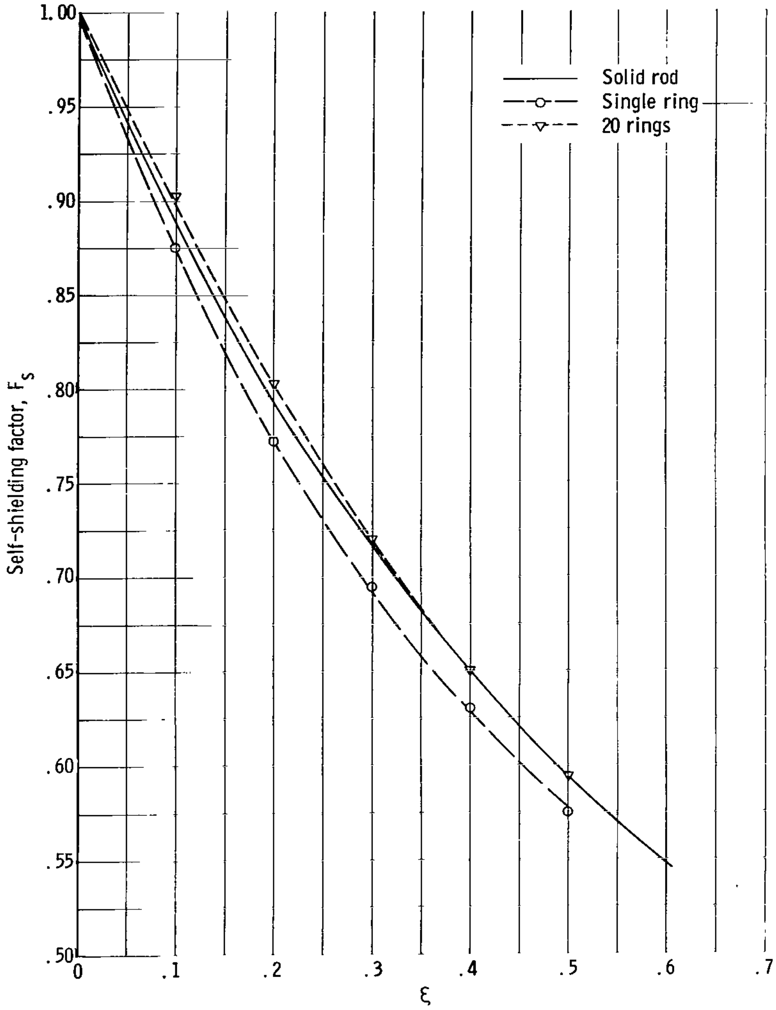

Figure 6. - Self-shielding factors for multiple cylindrical configurations.

Blackness factors, rather than self-shielding factors, are plotted inasmuch as a simple representative value of ξ over an entire resonance cannot be obtained.

The blackness for an isotropic angular-flux distribution is compared with the blackness obtained using a cosine incident angular distribution. The isotropic distribution is introduced as a mathematical device to ascertain the effect of a change in angular distribution on the blackness factor averaged over a Breit-Wigner resonance line shape and a $1/E$ energy spectrum.

The change in blackness is more sensitive to an isotropic incident flux than to a cosine incident flux, as shown in figure 7, for smaller numbers of annuli. The greatest difference between the cosine angular and the isotropic angular-incident-flux distributions occurs for a single annulus, but the so-

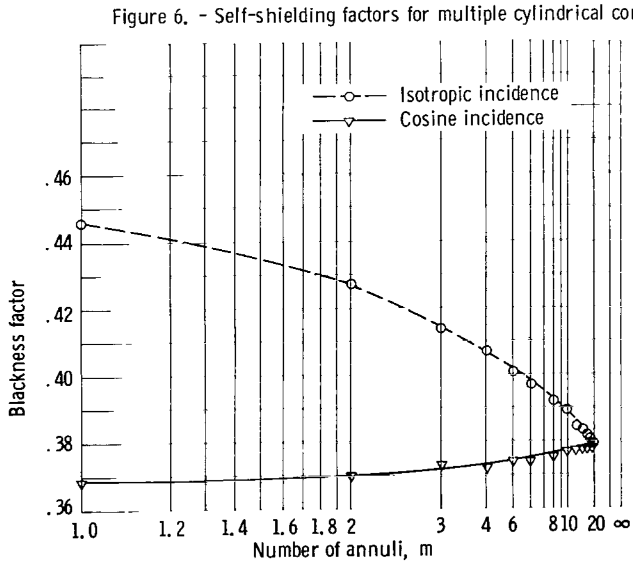

Figure 7. - Blackness factor plotted against number of annuli over a resonance.

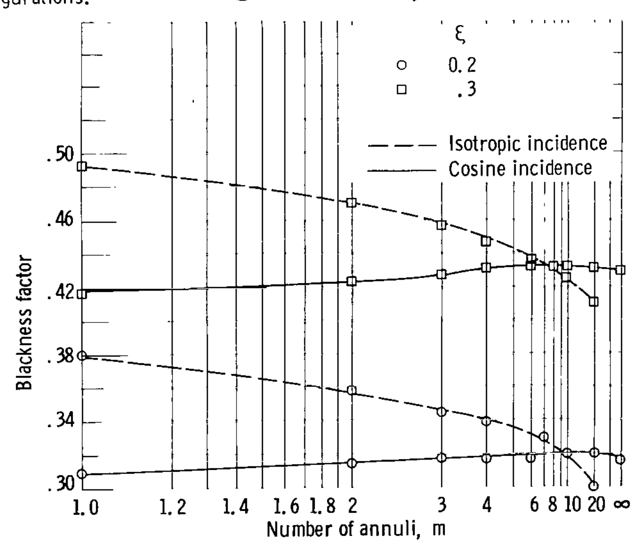

Figure 8. - Blackness factors plotted against number of annuli for monoenergetic flux.

lution appears to converge for large numbers of concentric cylinders. In order to ascertain whether this apparent convergence is real, monoenergetic blackness factors are computed and are shown in figure 8. These results indicate that, if the resonance calculations had been done for a larger number of annuli, the blackness factor curves would cross.

Lewis Research Center
National Aeronautics and Space Administration
Cleveland, Ohio, July 29, 1964

APPENDIX A

DERIVATION OF ANGULAR DISTRIBUTIONS

The results of the following derivation were used to obtain an isotropic neutron-angular-flux distribution. A differential element of area dA in spherical coordinates can be written

$$dA = r^2 \sin \Phi \, d\Phi \, d\theta$$

If $r = 1$ and polar coordinates are used, the following identities may be introduced (see fig. 9):

$$u \equiv \cos \alpha$$

$$v \equiv \cos \beta$$

$$w \equiv \cos \Upsilon$$

(a) Polar coordinate system. (b) Cartesian coordinate system.

Figure 9. - Coordinate systems.

By simple transformation,

$$r = \rho = 1 \qquad d\Phi = d\Upsilon$$

$$\Upsilon = \Phi \qquad d\theta = dv$$

$$v = \cos \beta = \theta \qquad dw = -\sin \Phi \, d\Phi$$

$$w = \cos \Phi$$

and

$$dA = \sin \Phi \, d\Phi \, d\theta = -dw \, dv$$

The probability density function of w, $p(w)\,dw$ can be written

$$p(w)\,dw = \frac{2\pi r^2 \sin \Phi \, d\Phi}{4\pi r^2} = -\frac{1}{2} \sin \Phi \, d\Phi = \frac{1}{2}\,dw \tag{A1}$$

If N_r is a random number, the solution of equation (A1) gives the method of choosing w for an isotropic distribution

$$N_r = \int_{-1}^{w} \frac{1}{2}\,dw' = \frac{1}{2}\,w' \Big|_{-1}^{w} = \frac{1}{2}(w + 1)$$

and

$$w = 2N_r - 1$$

Thus w of the set u, v, and w can be selected.

Since $\vec{\Phi}_u$ is orthogonal to the vector $\vec{\theta}_u$, θ can be obtained independently. The fact that θ may range from $-\pi$ to π with equiprobability means the value of θ can be determined in the following manner:

$$N_r = \int_{-\pi}^{\theta} P(\theta')d\theta' = \int_{-\pi}^{\theta} \frac{d\theta'}{2\pi} = \frac{1}{2\pi}(\theta + \pi)$$

and

$$\theta = \pi(2N_r - 1)$$

A cosine distribution may be gained by the following substitution:

$$p(w) = 2w$$

by definition and

$$p(w)\ dw = 2w\ dw$$

Let

$$N_r = \int_0^w 2w'\ dw' = w^2$$

Hence

$$w = \sqrt{N_r}$$

APPENDIX B

DERIVATION OF NEUTRON PATH LENGTH IN MATERIAL

The equation used to calculate the path length in material shall be derived in this appendix. First consider the section at a cutting plane perpendicular to the infinite hollow rod (see fig. 10). This figure is composed of two concentric circles A and B with radii R_1 and R_2, respectively, as well as the projection into the cutting plane of a neutron trajectory A'A".

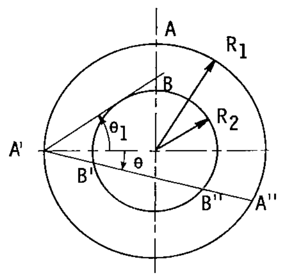

Figure 10. - Section at cutting plane.

The distance A'A" must first be obtained, and then the distance B'B" subtracted. Choosing the point A' as the origin of the coordinate system and writing the equation for A'A" in terms of R_1 and θ result in the following equation:

$$A'A" = 2R_1 \cos \theta \tag{B1}$$

The equation for the circle B in terms of R_1, R_2, and θ is

$$R_2^2 = r^2 + R_1^2 - 2rR_1 \cos \theta \tag{B2}$$

where (r,θ) is the polar vector that describes the circle B' from A', the origin. Solving for r gives

$$r = R_1 \cos \theta \pm \sqrt{R_1^2 \cos^2 \theta - (R_1^2 - R_2^2)} \tag{B3}$$

Since $\cos^2\theta - 1 = -\sin^2\theta$,

$$r = R_1 \cos \theta \pm \sqrt{R_2^2 - R_1^2 \sin^2\theta} \tag{B4}$$

which describes the circle B. Hence

$$B'B" = 2\sqrt{R_2^2 - R_1^2 \sin^2\theta} \tag{B5}$$

Thus the expression for the projection of the path length on the cutting plane is

$$2R_1 \cos \theta - 2 \sqrt{R_2^2 - R_1^2 \sin^2\theta} \tag{B6}$$

When the projection intersects an inner rod or annulus, the following expressions (which may be obtained from eq. (B5)) are used (see fig. 11):

$$C'C" = 2 \sqrt{R_3^2 - R^2 \sin^2\theta} \tag{B7}$$

$$D'D'' - E'E'' = 2\left(\sqrt{R_5^2 - R^2 \sin^2\theta} - \sqrt{R_4^2 - R^2 \sin^2\theta}\right) \tag{B8}$$

Once the length of the entire projection λ_p (on the material in the cutting plane) has been computed, the chord length λ is calculated by the following formula:

$$\lambda = \frac{\lambda_p}{\cos \Phi}$$

where Φ is the angle the neutron velocity vector makes with the cutting plane.

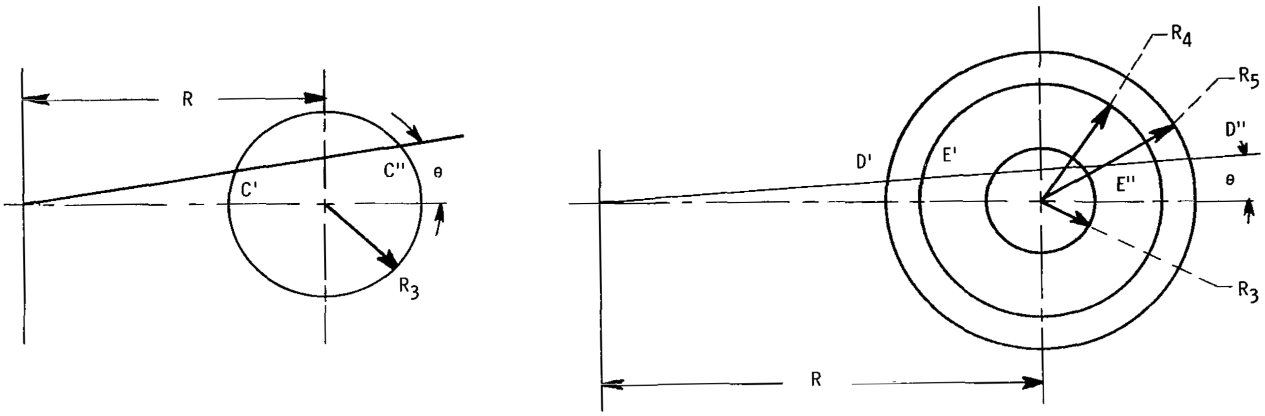

Figure 11. - Projection of neutron trajectories through various configurations.

REFERENCES

1. Sauer, A.: Approximate Escape Probabilities. Nuclear Sci. Eng., vol. 16, no. 3, July 1963, pp. 329-335.

2. Creutz, E., Jupnik, H., Snyder, T., and Wigner, E. P.: Effect of Geometry on Resonance Absorption of Neutrons by Uranium. Jour. Appl. Phys., vol. 26, no. 3, Mar. 1955, pp. 271-275.

3. Cashwell, E. D., and Everett, C. J.: A Practical Manual on the Monte Carlo Method for Random Walk Problems. LA-2120, AEC, 1957.

4. Hughes, Donald J., and Schwartz, Robert B.: Neutron Cross Sections. Second ed., BNL-325, AEC, 1958.

5. Weinberg, Alvin Martin, and Wigner, Eugene P.: The Physical Theory of Neutron Chain Reactors. Univ. Chicago Press, 1958, pp. 73-79; 161-167.

6. Argonne National Laboratory: Reactor Physics Constants. ANL-5800, AEC, 1958, pp. 387-392.

7. Dwork, J., Hofmann, P. L., Hurwitz, H., Jr., and Clancy, E. F.: Self-Shielding Factors for Infinitely Long, Hollow Cylinders. KAPL-1262, AEC, 1955.

8. Hald, Anders: Statistical Theory with Engineering Applications. John Wiley & Sons, Inc., 1957, pp. 668-713.

9. Case, K. M., de Hoffmann, F., and Placzek, G.: Introduction to the Theory of Neutron Diffusion. Vol. I. U.S. Govt. Printing Office, Wash., D.C., 1953.

NASA-Langley, 1964 E-2504

"The aeronautical and space activities of the United States shall be conducted so as to contribute . . . to the expansion of human knowledge of phenomena in the atmosphere and space. The Administration shall provide for the widest practicable and appropriate dissemination of information concerning its activities and the results thereof."

—NATIONAL AERONAUTICS AND SPACE ACT OF 1958

NASA SCIENTIFIC AND TECHNICAL PUBLICATIONS

TECHNICAL REPORTS: Scientific and technical information considered important, complete, and a lasting contribution to existing knowledge.

TECHNICAL NOTES: Information less broad in scope but nevertheless of importance as a contribution to existing knowledge.

TECHNICAL MEMORANDUMS: Information receiving limited distribution because of preliminary data, security classification, or other reasons.

CONTRACTOR REPORTS: Technical information generated in connection with a NASA contract or grant and released under NASA auspices.

TECHNICAL TRANSLATIONS: Information published in a foreign language considered to merit NASA distribution in English.

TECHNICAL REPRINTS: Information derived from NASA activities and initially published in the form of journal articles.

SPECIAL PUBLICATIONS: Information derived from or of value to NASA activities but not necessarily reporting the results of individual NASA-programmed scientific efforts. Publications include conference proceedings, monographs, data compilations, handbooks, sourcebooks, and special bibliographies.

Details on the availability of these publications may be obtained from:

SCIENTIFIC AND TECHNICAL INFORMATION DIVISION

NATIONAL AERONAUTICS AND SPACE ADMINISTRATION

Washington, D.C. 20546